Microtubule Protein ADP-Ribosylation in Vitro Leads to Assembly Inhibition and Rapid Depolymerization†

Robin M. Scaife,‡ Leslie Wilson,*,§ and Daniel L. Purich‖

Fred Hutchinson Cancer Research Center, Seattle, Washington 98104, Department of Biological Sciences, University of California, Santa Barbara, California 93106, and Department of Biochemistry and Molecular Biology, University of Florida College of Medicine, Gainesville, Florida 32610

Received July 15, 1991; Revised Manuscript Received September 26, 1991

ABSTRACT: Bovine brain microtubule protein, containing both tubulin and microtubule-associated proteins, undergoes ADP-ribosylation in the presence of [^{14}C]NAD$^+$ and a turkey erythrocyte mono-ADP-ribosyltransferase in vitro. The modification reaction could be demonstrated in crude brain tissue extracts where selective ADP-ribosylation of both the α and β chains of tubulin and of the high molecular weight microtubule-associated protein MAP-2 occurred. In experiments with purified microtubule protein, tubulin dimer, the high molecular weight microtubule-associated protein MAP-2, and another high molecular weight mirotubule-associated protein which may be a MAP-1 species were heavily labeled. Tubulin and MAP-2 incorporated [^{14}C]ADP-ribose to an average extent of approximately 2.4 and 30 mol of ADP-ribose/mol of protein, respectively. Assembly of microtubule protein into microtubules in vitro was inhibited by ADP-ribosylation, and incubation of assembled steady-state microtubules with ADP-ribosyltransferase and NAD$^+$ resulted in rapid depolymerization of the microtubules. Thus, the eukaryotic enzyme can ADP-ribosylate tubulin and microtubule-associated proteins to much greater extents than previously observed with cholera and pertussis toxins, and the modification can significantly modulate microtubule assembly and disassembly.

Mono-ADP-ribosylation is a posttranslational covalent modification of proteins (Ueda & Hayaishi, 1985) that is catalyzed by certain bacterial toxins (Raeburn et al., 1968; Moss & Vaughan, 1978; Aktories et al., 1986) and a number of eukaryotic enzymes (Lee & Iglewski, 1984; Moss et al., 1980). These enzymatic activities transfer an ADP-ribose moiety from NAD$^+$ to arginine, cysteine, or diphthamide (modified histidine) residues of protein substrates. The ability to serve as a substrate for mono-ADP-ribosylation in vitro appears to be a characteristic property of GTP-binding proteins. For example, the G_i and G_s regulatory subunits of adenylate cyclase (Cassel & Pfeuffer, 1978; Gill & Meren, 1978; Moss & Richardson, 1978; Tanuma et al., 1989), the α subunit of the regulatory retinal protein transducin (Abood et al., 1982), elongation factor 2 (Cooper et al., 1981; Fendrick & Iglewski, 1989), and the proto-oncogene Ha-ras (Tsai et al., 1985) all are substrates in vitro for ADP-ribosyltransferases.

Mono-ADP-ribosyltransferases have been isolated from cytosolic, membrane, and nuclear fractions of turkey erythrocytes (West & Moss, 1986), and ADP-ribosyltransferase activities have been identified in a variety of animal tissues including brain (De Wolff et al., 1981; Richter et al., 1983; Bernofsky & Amamoo, 1984; Soman et al., 1984; Tanigawa et al., 1984; Leno & Ledford, 1989; Brune & Lapetina, 1989; Fendrick & Iglewski, 1989). Although elongation factor 2 can serve as a substrate for diphthamide-specific endogenous mono-ADP-ribosyltransferases in cells (Fendrick & Iglewski, 1989), no substrates for the arginine- and cysteine-specific eukaryotic ADP-ribosyltransferases have been identified in cells, and the biological functions of mono-ADP-ribosylation reactions in eukaryotes remain poorly understood. However, a role for reversible mono-ADP-ribosylation in the regulation of a 78-kDa glucose-sensitive and heat shock sensitive protein (GRP78) in eukaryotes (Carlsson & Lazarides, 1983) and of dinitrogenase reductase in certain prokaryotes has been demonstrated recently (Leno & Ledford, 1989; Hendershot et al., 1988; Luddon & Roberts, 1989).

Tubulin is a GTP-binding protein, and primary sequence data indicate several regions of homology with other GTP-binding proteins (Sternlicht et al., 1987). Both α- and β-tubulin subunits and high molecular weight microtubule-associated proteins (HMW-MAPs)[1] have been identified as substrates in vitro for ADP-ribosylation by cholera toxin (Kaslow et al., 1981; Amir-Zaltsman et al., 1982; Hawkins & Browning, 1982) and pertussis toxin (Lim et al., 1985). However, the levels of ADP-ribosylation achieved with these toxins were very substoichiometric (e.g., in one study, no more than 0.1% of the tubulin could be ADP-ribosylated; Amir-Zaltsman et al., 1982), and we have found that the low-level ADP-ribosylation of bovine brain microtubule protein that occurs with these toxins does not affect polymerization of the protein into microtubules in vitro (unpublished data). We report here that bovine brain α- and β-tubulin polypeptides and HMW-MAPs are substrates for ADP-ribosylation in vitro by a eukaryotic NAD:arginine ADP-ribosyltransferase. The reaction is highly selective for tubulin and HMW-MAPs in crude brain extracts, and the levels of modification are 2 orders of magnitude higher than those observed with bacterial toxins. ADP-Ribosylation results in inhibition of microtubule assembly and microtubule depolymerization, suggesting that ADP-

† Supported by USPHS Grant NS13560 from the National Institute of Neurological and Communicative Disorders and Stroke.

‡ Fred Hutchinson Cancer Research Center.
§ University of California, Santa Barbara.
‖ University of Florida College of Medicine.

[1] Abbreviations: HMW-MAPs, high molecular weight microtubule-associated proteins; MME buffer, 100 mM 2-(*N*-morpholino)ethanesulfonic acid, pH 6.8, 1 mM $MgSO_4$, and 1 mM EGTA; TCA, trichloroacetic acid.

0006-2960/92/0431-310$03.00/0

ribosylation of tubulin and/or the HMW-MAPs may play a role in the regulation of microtubule polymerization or function.

Materials and Methods

Isolation of Bovine Brain Tubulin and HMW-MAPs, Gel Electrophoresis, and Blotting. Bovine brain microtubule protein was obtained by cycles of assembly and disassembly in vitro (Margolis et al., 1986). Tubulin and the HMW-MAPs were separated by phosphocellulose chromatography in MME buffer [100 mM 2-(*N*-morpholino)ethanesulfonic acid, pH 6.8, 1 mM $MgSO_4$, and 1 mM EGTA] (Williams & Detrich, 1979). Unless stated otherwise, SDS–PAGE was performed with 7% polyacrylamide gels as described by Laemmli (1970). Proteins were visualized with Coomassie Blue. Autoradiograms of gels were obtained after treatment of gels with 2,5-diphenyloxazole (PPO). Electrophoretic blotting was carried out as described by Towbin et al. (1979). Antigen on blots was visualized by autoradiography after exposure to ^{125}I-labeled protein A. Two-dimensional PAGE was carried out by the procedure of O'Farrell (1975).

Quantitation of [^{14}C]NAD$^+$ Incorporation into Proteins. Incorporation of radiolabel from [^{14}C]NAD$^+$ into tubulin and MAP-2 was quantitated by liquid scintillation counting of trichloroacetic acid (TCA) precipitated protein, or by quantitative phosphorimager analysis. TCA precipitation was performed by adding 10 μL of a 25% solution of TCA (w/v) to 10 μL of protein solution. Samples were incubated at 4 °C for 30 min and centrifuged at 4 °C for 10 min at 14000*g*. Pellets were washed twice with 300-μL volumes of 8% TCA (w/v) and then solubilized in 1% SDS. Radioactivity was determined in a Beckman LS7000 liquid scintillation spectrometer. Background radioactivity was determined by TCA precipitation of 10-μL microtubule protein aliquots incubated with [^{14}C]NAD$^+$ in the absence of ADP-ribosyltransferase. The proportion of TCA-precipitable ^{14}C radiolabel incorporated into tubulin (α, β, α*, β*, see Figure 4) and MAP-2 was determined by densitometric analysis of autoradiograms derived from duplicate microtubule samples that had been electrophoresed on 7% polyacrylamide gels. Densitometry was performed using an LKB laser densitometer (ULTROSCAN 2202). Quantitation of radiolabel incorporation into tubulin and MAP-2 was also carried out in 7% SDS–polyacrylamide gels by phosphorimager analysis (Model 400A, Molecular Dynamics, Sunnyvale, CA) using [^{14}C]NAD$^+$-radiolabeled standards spotted on filter paper. Stoichiometries of ADP-ribosylation were based on molecular masses of 100 kDa for tubulin dimer and 200 kDa for MAP-2.

Miscellaneous Procedures and Materials. Electron micrographs of taxol-polymerized microtubules were obtained by negative staining with uranyl acetate after diluting the microtubule suspensions into MME buffer containing 50% sucrose. Microtubule polymerization and depolymerization were determined by turbidimetry at 350 nm, using a Cary 219 spectrophotometer (equipped with a thermostatically controlled cuvette holder, equilibrated at 30 °C). Analytical centrifugation was performed with a Beckman TL-100, ultracentrifuge, and samples were routinely centrifuged through density cushions of 20% glycerol in MME buffer.

Electrophoresis reagents were obtained from Bio-Rad. Monoclonal anti-tubulin antisera and [U-^{14}C]NAD$^+$ (270 mCi/mol) were obtained from Amersham. Phosphocellulose was purchased from Whatman, and taxol was a gift from Dr. M. Suffness, Natural Products Branch, National Cancer Institute, NIH. Turkey erythrocyte ADP-ribosyltransferase A was generously provided by Dr. Joel Moss, National Institutes of Health, as a solution in 50% propylene glycol/50 mM sodium phosphate, pH 7.0. All other reagents were from Sigma Chemical Co.

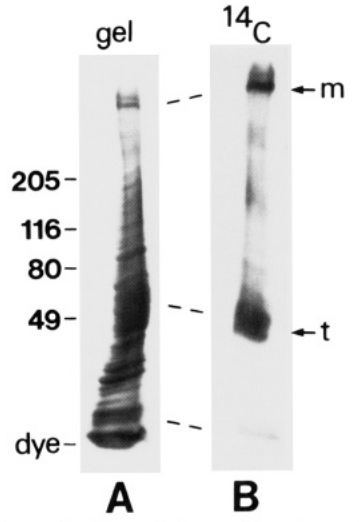

FIGURE 1: Polyacrylamide gel electrophoresis analysis of ADP-ribosylated brain tissue extracts. Brain tissue was homogenized in MME buffer, and a supernatant solution containing 12 mg/mL total protein was obtained by centrifugation at 20000*g* for 20 min at 4 °C (Margolis et al., 1986). After addition of protease inhibitors to 50 μL of the solution of soluble brain proteins (1 mM phenylmethanesulfonyl fluoride, 10 μg/mL *N*-tosyl-L-phenylalanine chloromethyl ketone, 1.8 mg/mL benzamidine, 2 μg/mL leupeptin, 1.5 mg/mL aprotinin, and 200 μg/mL pepstatin), the solution was incubated for 30 min at 30 °C with 6 μg/mL erythrocyte ADP-ribosyltransferase and 0.1 mM [^{14}C]NAD$^+$ (16.6 mCi/mmol). The sample was then boiled in SDS and subjected to electrophoresis on a 5–12% polyacrylamide gel. (A) Coomassie Blue stained gel; (B) autoradiogram. Molecular mass marker positions are indicated in kilodaltons. The position on the autoradiogram of α- and β-tubulin is denoted by t, and the position of MAP-2 is denoted by m.

Results

ADP-Ribosylation of Tubulin and HMW-MAPs. ADP-Ribosylation of tubulin and HMW-MAPs occurred selectively upon incubation of crude bovine brain supernatant extracts with turkey erythrocyte mono-ADP-ribosyltransferase and radiolabeled NAD$^+$. These conditions were comparable to those used in earlier ADP-ribosylation studies with cholera and pertussis toxins as the ADP-ribosyltransferases (Kaslow et al., 1981; Amir-Zaltsman et al., 1982; Hawkins & Browning, 1982). Electrophoresis and subsequent autoradiography of an SDS–PAGE gel of the reaction products (Figure 1) demonstrated strong radiolabeling of two protein species of molecular mass approximately 50–55 kDa and a high molecular weight protein species of approximately 300K. These radiolabeled species were identified as α- and β-tubulin and MAP-2 based upon their migration on two-dimensional gels (data not shown). Relatively few of the numerous protein species present in the crude brain extract were labeled, and only α- and β-tubulin and MAP-2 were radiolabeled to significant extents. Thus, the eukaryotic ADP-ribosyltransferase, like cholera toxin (Kaslow et al., 1981; Amir-Zaltsman et al., 1982; Hawkins & Browning, 1982), acts selectively to modify tubulin and MAP-2 in the presence of many other potentially reactive proteins.

The relationship between the quantity of transferase and ADP-ribosylation of α- and β-tubulin and MAP-2 was determined by adding the transferase to purified microtubule protein in the presence of radiolabeled NAD$^+$ (Table I). Maximal ADP-ribosylation occurred at approximately 6 μg/mL transferase, and amounted to approximately 2.4 mol

Table I: ADP-Ribosylation of Bovine Brain Tubulin and MAP-2[a]

transferase concn (μg/mL)	mol of ADP-ribose/mol of tubulin	mol of ADP-ribose/mol of MAP-2
30.0	2.43 (±0.17)	30.7 (±1.8)
6.0	2.39 (±0.22)	30.4 (±2.9)
3.0	1.50 (±0.10)	19.1 (±1.3)
1.5	0.92 (±0.11)	11.9 (±1.4)
0.6	0.63 (±0.10)	8.0 (±1.4)
0.3	0.38 (±0.03)	4.8 (±0.28)

[a] Aliquots (10 μL) of purified microtubule protein (1.5 mg/mL) in MME buffer were incubated with [^{14}C]NAD$^+$ (0.1 mM, 16.6 mCi/mmol) and the indicated concentrations of turkey erythrocyte ADP-ribosyltransferase for 30 min at 30 °C. Radioactivity was determined after precipitating the proteins with trichloroacetic acid (see Materials and Methods). The results shown are from three determinations with the same enzyme and microtubule protein preparations. The values in parentheses are the standard deviations.

of ADP-ribose/mol of tubulin and 30 mol of ADP-ribose/mol of MAP-2.

Effects of ADP-Ribosylation of Microtubule Protein on Microtubule Polymerization and Depolymerization in Vitro. Polymerization of microtubule protein into microtubules was monitored after incubating purified microtubule protein with two different ratios of ADP-ribosyltransferase to microtubule protein on a weight to weight basis (Figure 2A). Polymerization was inhibited 60% at a microtubule protein:enzyme ratio of 6000:1 (curve b), and it was completely inhibited at a microtubule protein to enzyme ratio of 3000:1 (curve c). Neither NAD$^+$ alone nor enzyme alone caused detectable inhibition of assembly (data not shown). Inclusion of the microtubule assembly-promoting agent taxol (50 μM) at a 3000:1 ratio of microtubule protein to enzyme overcame the inhibition (curve c + taxol). Microtubules polymerized in the presence of the ADP-ribosyltransferase and taxol displayed normal morphology as judged by negative-stain electron microscopy (Figure 2B) and were the only product of taxol-induced assembly discernible by electron microscopy.

To determine whether ADP-ribosylated tubulin could incorporate into microtubules, purified tubulin was ADP-ribosylated with [^{14}C]NAD$^+$. The ADP-ribosylated tubulin was then added to unmodified and unfractionated microtubule protein, and the mixture was polymerized. Microtubules were separated from soluble microtubule protein by centrifugation through 20% glycerol cushions, and the microtubule pellets (lanes 2, 4, and 6) and the soluble microtubule proteins (lanes 1, 3, and 5) were analyzed on polyacrylamide gels by Coomassie Blue staining (Figure 3A) and autoradiography (Figure 3B). Radiolabeled tubulin was found in the microtubule pellet (Figure 3B, lane 4), indicating that some of the ADP-ribosylated tubulin was assembly-competent. However, relative to the distribution between the soluble and microtubule fractions of unmodified tubulin, the radiolabeled tubulin was enriched in the soluble fraction (Figure 3B, lane 3) (compare lanes 3 and 4 in panel B with lanes 3 and 4 in panel A). These results suggest that the ability of ADP-ribosylated tubulin to be incorporated into microtubules was diminished as compared with that of unmodified tubulin.

Essentially all of the radiolabeled tubulin was recovered in the microtubule pellet when polymerization was carried out in the presence of 50 μM taxol (compare lanes 5 and 6), indicating that the presence of taxol overcame the diminished ability of ADP-ribosylated tubulin to be incorporated into microtubules. Control experiments were carried out under nonassembling conditions, achieved by enzymatically depleting GTP (lanes 1 and 2). Under these conditions as expected, all of the tubulin (labeled and unlabeled) was found in the unassembled fraction (lane 1).

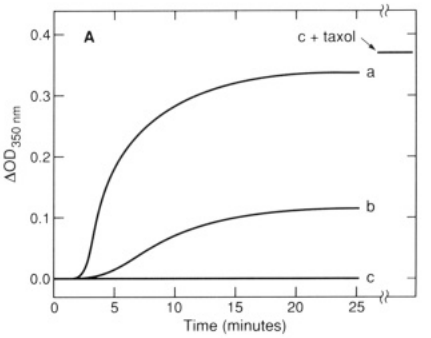

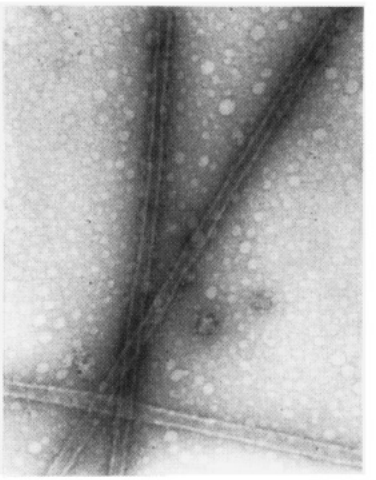

B

FIGURE 2: Inhibition of microtubule assembly by ADP-ribosylation. (A) Aliquots (300 μL) of purified microtubule protein (1.8 mg/mL) in MME buffer were incubated without (curve a) or with (curves b and c) erythrocyte ADP-ribosyltransferase and NAD$^+$ (0.11 mM) for 30 min at 30 °C and then cooled to 4 °C (to depolymerize any microtubule protein structures that may have formed at 30 °C). After addition of GTP (final concentration 0.125 mM), samples were incubated at 30 °C in quartz cuvettes, and turbidity was recorded at 350 nm. Assembly curves b and c were obtained with 0.3 μg/mL ADP-ribosyltransferase (6000:1, microtubule protein to enzyme, w/w) and 0.6 μg/mL ADP-ribosyltransferase (3000:1, microtubule protein to enzyme, w/w), respectively. Taxol (final concentration, 50 μM) was added to a fourth cuvette containing 0.6 μg/mL ADP-ribosyltransferase (3000:1, microtubule protein to enzyme, w/w) (curve c + taxol). (B) Electron micrograph of taxol-treated microtubule protein after incubation with NAD$^+$ (0.1 mM) in the presence of a 3000:1 ratio (w/w) of ADP-ribosyltransferase and microtubule protein (from curve c + taxol, panel A). Magnification = 84000×.

Several ^{14}C-radiolabeled species were evident on the autoradiogram that were not detectable by staining (M_r 60–70K). By immunoblotting with antisera to both α- and β-tubulin, it appeared that at least two of the additional radiolabeled species were low-mobility ADP-ribosylated forms of tubulin (Figure 4). None of these bands were labeled with antisera to both α- and β-tubulin. Therefore, the bands do not appear to represent chemically cross-linked αβ tubulin dimers. The pronounced effect of ADP-ribosylation on the electrophoretic mobility of these α- and β-tubulin species does not impair their ability to undergo taxol-dependent assembly into microtubules (Figure 3B, lanes 5 and 6). ADP-Ribosylation of Ha-ras and GRP78 similarly results in a decrease in mobility on SDS–PAGE (Tsai et al., 1985; Leno & Ledford, 1989). The other M_r 60–70K proteins have not yet been identified. However, bovine brain microtubule proteins prepared by cycles of polymerization and depolymerization in vitro contain small quantities of tau proteins which migrate on SDS gels as four to five distinct protein bands of M_r 60–70K, and some of the

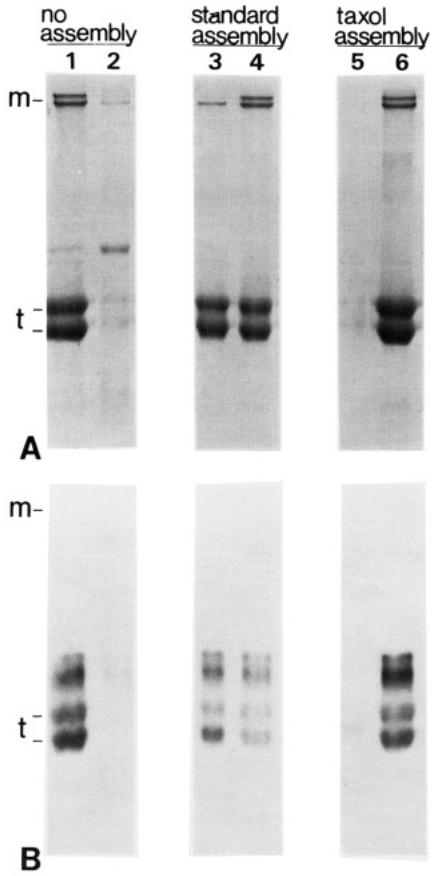

FIGURE 3: Assembly properties of ADP-ribosylated tubulin. Purified tubulin (1.2 mg/mL) in MME buffer was incubated with the erythrocyte enzyme (2 μg/mL) and [^{14}C]NAD$^+$ (0.05 mM, 41.6 mCi/mmol) for 30 min at 30 °C. After dialysis into MME buffer (4 °C, 150 min), 5-μL samples of the resulting solution were combined with 12-μL aliquots of purified unfractionated microtubule protein (6 mg/mL), containing 1 mM thymidine, which completely inhibited the transferase as indicated by the absence of radiolabel in the MAP-2 fraction. Samples were incubated at 30 °C for 30 min (either under assembly-promoting or under assembly-inhibiting conditions) and centrifuged at 150000g for 45 min through 20-μL cushions of 20% glycerol in MME buffer. Supernatant fractions (lanes 1, 3, and 5) and pellet fractions (lanes 2, 4, and 6) were electrophoresed, the gel was stained with Coomassie Blue (panel A), and a duplicate gel was processed for incorporation of radiolabel by autoradiography (panel B). For the no-assembly control sample (lanes 1 and 2), assembly was inhibited by fructose 6-phosphate (8 mM) and phosphofructokinase (3.3 enzyme units/mL); standard assembly (lanes 3 and 4) was achieved by addition of GTP (0.25 mM); taxol assembly (lanes 5 and 6) was achieved by adding 50 μM taxol in the presence of GTP (0.25 mM). t = α- and β-tubulin, m = HMW-MAPs.

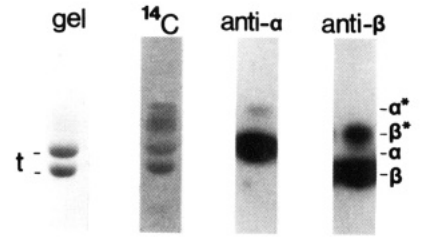

FIGURE 4: Effect of ADP-ribosylation on tubulin electrophoretic mobility. Purified microtubule protein in MME buffer (80 μL, 3 mg/mL) was incubated with turkey erythrocyte ADP-ribosyltransferase (3 μg/mL) and [^{14}C]NAD$^+$ (0.1 mM, 10 mCi/mmol) for 60 min at 30 °C and then boiled in SDS. Samples were electrophoresed, and the Coomassie Blue stained gel was processed for autoradiography (Materials and Methods). Duplicate gels were blotted and probed with anti-α-tubulin and anti-β-tubulin antisera. The positions of α- and β-tubulin (t) and the two antigenic species (M_r = 60–70K, α* and β*) are indicated. Only the tubulin region of the gel, autoradiogram, and blots are shown.

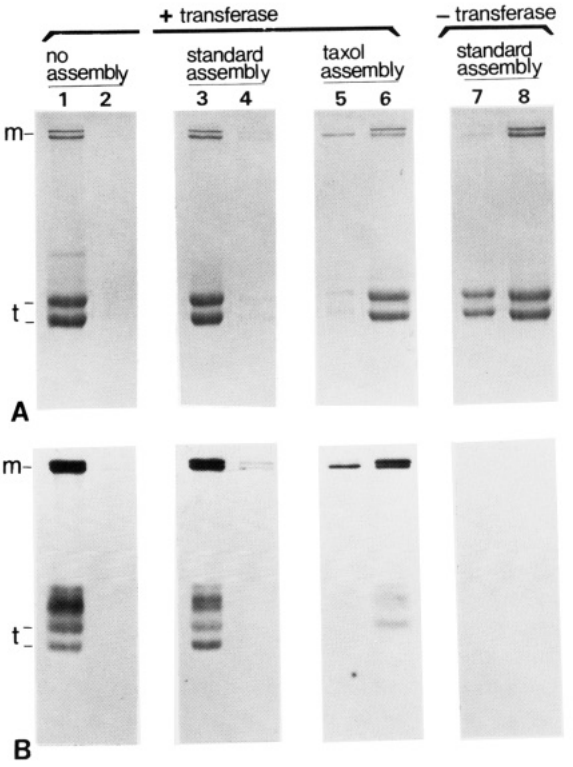

FIGURE 5: ADP-Ribosylation of assembled microtubule proteins. Aliquots (15 μL) of purified microtubule protein (6 mg/mL) in MME buffer were incubated at 30 °C for 30 min under assembly-promoting or assembly-inhibiting conditions (see legend to Figure 4), followed by incubation with erythrocyte ADP-ribosyltransferase (3 μg/mL) and [^{14}C]NAD$^+$ (0.1 mM, 8.3 mCi/mmol) for an additional 30 min at 30 °C. Samples were then centrifuged at 150000g for 45 min through 20-μL cushions of 20% glycerol in MME buffer. Supernatant fractions (lanes 1, 3, 5, and 7) and microtubule pellet fractions (lanes 2, 4, 6, and 8) were analyzed on a gel by Coomassie Blue staining (panel A) and by autoradiography (panel B). For the no-assembly control sample (lanes 1 and 2), assembly was inhibited by fructose 6-phosphate (8 mM) and phosphofructokinase (3.3 enzyme units/mL); standard assembly (lanes 3 and 4) corresponds to assembly promoted by GTP (0.25 mM) with ADP-ribosyltransferase and NAD$^+$ added after assembly had reached steady state; taxol assembly (lanes 5 and 6) corresponds to assembly promoted by addition of 50 μM taxol in the presence of GTP (0.25 mM), with ADP-ribosyltransferase and NAD$^+$ added after assembly had reached steady state. A control is also shown (lanes 7 and 8), corresponding to standard assembly promoted with GTP (0.25 mM), but enzyme buffer (see Materials and Methods) added instead of the erythrocyte enzyme. t = α- and β-tubulins, m = HMW-MAPs.

radiolabeled species in this region of the gel may represent ADP-ribosylated tau.

To determine whether tubulin and HMW-MAPs in microtubules were substrates for the ADP-ribosyltransferase and whether ADP-ribosylation might destabilize the microtubules, microtubule protein was assembled to polymer-mass steady-state prior to addition of ADP-ribosyltransferase and radiolabeled NAD$^+$. After incubation with enzyme for 30 min at 30 °C, microtubules were collected by centrifugation, and both soluble (lanes 1, 3, 5, and 7) and microtubule pellet fractions (lanes 2, 4, 6, and 8) were analyzed on a gel by Coomassie Blue staining (Figure 5A) and autoradiography (Figure 5B). The microtubule protein was found only in the supernatant fraction (Figure 5A, compare lanes 3 and 4). Thus, assembled microtubules appeared to depolymerize upon incubation with the ADP-ribosyltransferase. In control experiments, all of the microtubule protein was in the supernatant fraction when microtubule protein was incubated under conditions of GTP depletion (Figure 5A, lanes 1 and 2), and most of the protein was found in the microtubule pellet as expected under as-

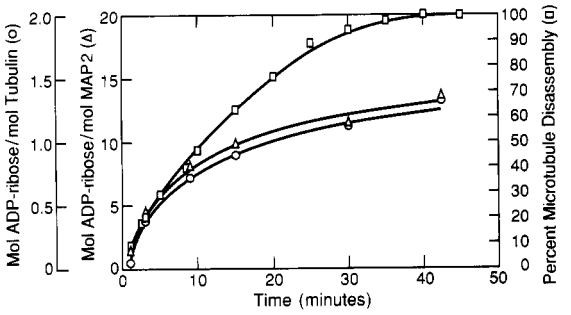

FIGURE 6: Disassembly of microtubules by ADP-ribosylation. Microtubule protein (450 μL, 1.5 mg/mL) in MME buffer was assembled to steady state with 0.1 mM GTP (30 min, 30 °C). [^{14}C]NAD$^+$ (0.1 mM, 16.6 mCi/mmol) and erythrocyte ADP-ribosyltransferase (1.5 μg/mL) were added (zero-time), and aliquots (20 μL) were removed at the indicated times at 30 °C, boiled in SDS, and electrophoresed on 5% polyacrylamide gels. Radiolabeling of tubulin (circles) and MAP-2 (triangles) was determined by phosphorimager analysis, and microtubule diassembly was determined by turbidimetry at 350 nm (squares). Neither addition of buffer containing propylene glycol (the vehicle for the ADP-ribosyltransferase) nor addition of the transferase without NAD$^+$ had any effect on the extent of assembly (data not shown).

sembly-promoting conditions (Figure 5A, lanes 7 and 8).

When assembled microtubules were polymerized in the presence of 50 μM taxol prior to incubation with the transferase and radiolabeled NAD$^+$, nearly all the microtubule protein was recovered in the polymerized fraction (Figure 5A, lane 6). Radiolabeling of α-tubulin and the HMW-MAPs in the microtubule pellet was apparent, but not β-tubulin (Figure 5B, lane 6). However, as compared with unassembled microtubule protein (Figure 5B, lane 1), the taxol-assembled α-tubulin and to a lesser extent the HMW-MAPs (Figure 5B, lane 6) were relatively poor substrates for the ADP-ribosyltransferase.

To further investigate the effects of ADP-ribosylation on microtubule depolymerization, the rate of depolymerization was monitored turbidimetrically after adding the transferase to microtubule protein that previously had been assembled to polymer-mass steady-state in the presence of NAD$^+$ (1000:1 ratio of microtubule protein to transferase). Using [^{14}C]-NAD$^+$, the levels of tubulin and MAP-2 ADP-ribosylation were also determined at various times during depolymerization (Figure 6). The rate of ADP-ribosylation was rapid during the first 10 min. It then slowed to an approximately linear rate which persisted for 45 min. Disassembly displayed typical first-order kinetics (Figure 6, squares). Incubation for 40 min resulted in complete disassembly of the microtubules and incorporation of approximately 1.3 mol of ADP-ribose/mol of tubulin dimer and 12–13 mol of ADP-ribose/mol of MAP-2.

Discussion

We have found that bovine brain tubulin and HMW-MAPs are substrates in vitro for a turkey erythrocyte mono-ADP-ribosyltransferase and that the eukaryotic transferase selectively ADP-ribosylates tubulin and MAP-2 in crude supernatant fractions of brain homogenates. With purified microtubule protein (tubulin plus MAPs), tubulin can be ADP-ribosylated to a level of approximately 2.4 mol/mol of tubulin dimer. One of the major HMW-MAPs that is ADP-ribosylated appears to be MAP-2 based upon its mobility on one- and two-dimensional polyacrylamide gels. However, other high molecular weight MAPs are also labeled to detectable extents, and at least one additional HMW-MAP, possibly MAP-1, is labeled to a significant extent (Figures 3 and 5). The specific identities of these modified HMW-MAPs remain to be determined. MAP-2 can be ADP-ribosylated to very high levels when ADP-ribosylation is carried out with purified microtubule protein (approximately 30 mol/mol of MAP-2). The fact that a large number of sites on MAP-2 can be ADP-ribosylated using purified microtubule protein is puzzling, and may be interpreted as indicating that the ADP-ribosyltransferase lacks specificity. However, such an apparent lack of specificity contrasts strongly with the high degree of selectivity of the transferase when the reaction is carried out in brain extracts. MAP-2 also undergoes extensive phosphorylation (more than 30 mol of phosphate/mol of protein) both in vitro (Tsuyama et al., 1986) and in vivo (Tsuyama et al., 1987).

ADP-Ribosylation of tubulin and HMW-MAPs has been reported previously with cholera and pertussis toxins serving as ADP-ribosyltransferases (Kaslow et al., 1981; Amir-Zaltsman et al., 1982; Hawkins & Browning, 1982). However, the extent of ADP-ribosylation with the bacterial toxins is more than 2 orders of magnitude less than that observed with the eukaryotic transferase. While ADP-ribosylation by cholera and pertussis toxins has no discernible effect on microtubule protein polymerization in vitro (unpublished data), we found that assembly of microtubule protein into microtubules was greatly reduced following ADP-ribosylation by the eukaryotic enzyme (Figure 2). Further, addition of the enzyme to microtubules at polymer-mass steady-state caused depolymerization of the microtubules (Figure 6). Along with the observation that ADP-ribosylation of tubulin and/or HMW-MAPs occurred selectively in crude brain extracts, the finding that ADP-ribosylation markedly altered the polymerization properties of the proteins indicates that ADP-ribosylation of tubulin or the HMW-MAPs may have a functional role in the control of microtubule assembly dynamics in certain cells or tissues.

The mechanism by which ADP-ribosylated tubulin and/or HMW-MAPs affect microtubule dynamics is unknown and remains to be determined. A reasonable possibility is that the effects on microtubule polymerization are due in part to modification of tubulin, because purified ADP-ribosylated tubulin exhibited impaired ability to polymerize when added to unfractionated microtubule protein (Figure 3). One possibility is that inhibition of microtubule polymerization is related to the mechanism by which ADP-ribosylation influences the enzymatic properties of many oligomeric GTP-binding proteins, including adenylate cyclase, elongation factor 2, transducin, and Ha-Ras (Cassel & Pfeuffer, 1978; Gill & Meren, 1978; Abood et al., 1982; Tsai et al., 1985). The covalent attachment of an ADP-ribose moiety to these proteins inhibits GTP hydrolysis, thereby perturbing protein subunit interactions [see Gilman (1984) and Pfeuffer and Helmreich (1989) for reviews]. However, depolymerization of previously assembled microtubules is unlikely to be due to inhibition of the GTPase activity of tubulin in the core of the polymer, because all of the tubulin-bound E-site nucleotide in the core is already hydrolyzed to GDP [e.g., see Stewart et al. (1990)]. If a short region of GTP-liganded tubulin at the ends of a microtubule (i.e., a "GTP cap") stabilizes the polymer, inhibition of GTPase activity at the ends would be expected to stabilize rather than destabilize the microtubule.

Another interesting possibility is that destabilization of the microtubules results in part from ADP-ribosylation of MAP-2. MAP-2 is the major HMW-MAP present in the bovine brain microtubules used in this study, and probably plays a major role in the stabilization of these microtubules by MAPs [e.g., see Farrell et al. (1987)]. ADP-Ribosylation of MAP-2 could exert a profound effect on growing and shortening dynamics

of microtubules in neuronal cells. Analogously, another family of MAPs, the tau proteins, are abnormally phosphorylated in Alzheimer's lesions (Grundke-Iqbal et al., 1986), and phosphorylation of tau reduces its ability to stabilize microtubules in vitro (Lindwall & Cole, 1984).

ADP-Ribosylated HMW-MAPs still appear to remain associated with the tubulin polymer (Figure 5, lane 6). Interestingly, the HMW-MAPs are modified in an unknown fashion in amyotrophic lateral sclerosis, and the modification greatly reduces the ability of the MAPs to promote tubulin assembly while not interfering with their binding to microtubules in vitro (Margolis et al., 1988). Such behavior may be similar to what we have observed with ADP-ribosylated MAP-2. Although MAP-2 appears to be a major ADP-ribose acceptor protein other than tubulin for the avian enzyme in crude brain tissue extracts, the finding that it undergoes ADP-ribosylation is puzzling, because it has no known GTP-binding capability. However, a glucose-regulated and heat shock regulated protein, lacking any known GTP-binding properties, has been shown to undergo ADP-ribosylation in vivo (Carlsson & Lazarides, 1983; Leno & Ledford, 1989).

Demonstration of a physiological role for the ADP-ribosylation of microtubule proteins, if any, remains to be achieved. The avian erythrocyte may be a good system for examining this issue. Such nucleated red cells contain the ADP-ribosyltransferase used in our studies as well as an extensive microtubule network constituting the marginal band. We have found that chicken erythrocyte tubulin is itself a good substrate for the avian ADP-ribosyltransferase in vitro (N. Raffaelli and D. L. Purich, unpublished data). The chicken erythrocyte, however, lacks the neuron-specific MAP-2 as well as other known high molecular weight microtubule-associated proteins. In this regard, another system will be needed to search for intracellular ADP-ribosylation of MAPs. To our knowledge, no one has observed ADP-ribosylation of microtuble protein in vivo. This may be because ADP-ribosyltransferases are strictly regulated under normal physiological conditions, as suggested by Lee and Iglewski (1984). Nontheless, the search for ADP-ribosylated microtubule proteins may be especially fruitful in light of the findings presented in this report.

Acknowledgments

We are indebted to Dr. Joel Moss for providing us with turkey erythrocyte ADP-ribosyltransferase, and we also express our gratitude to Dr. Robert L. Margolis in whose laboratories several of these experiments were completed. We thank Dr. Mary Ann Jordan for critically reading and commenting on the manuscript.

Registry No. ADP-ribosyltransferase, 58319-92-9.

References

Abood, M. E., Hurley, J. B., Pappone, M. C., Bourne, H. R., & Stryer, L. (1982) *J. Biol. Chem. 257*, 10540–10543.

Aktories, K., Ankenbauer, T., Schering, B., & Jakobs, K. (1986) *Eur. J. Biochem. 161*, 155–162.

Amir-Zaltsman, Y., Ezra, E., Scherson, T., Zutra, A., Littauer, U. Z., & Salomon, Y. (1982) *EMBO J. 1*, 181–186.

Bernofsky, C., & Amamoo, D. G. (1984) *Biochem. Biophys. Res. Commun. 118*, 663–668.

Brune, B., & Lapetina, E. G. (1989) *J. Biol. Chem. 264*, 8455–8458.

Carlsson, L., & Lazarides, E. (1983) *Proc. Natl. Acad. Sci. U.S.A. 80*, 4664–4668.

Cassel, D., & Pfeuffer, T. (1978) *Proc. Natl. Acad. Sci. U.S.A. 75*, 2669–2673.

Cooper, D., Jagus, R., Somers, R., & Rodbell, M. (1981) *Biochem. Biophys. Res. Commun. 101*, 1179–1185.

De Wolff, M. J. S., Vittii, P., Ambesi-Impiombato, F. S., & Kohn, L. D. (1981) *J. Biol. Chem. 256*, 12287–12296.

Farrell, K. W., Jordan, M. A., Miller, H. P., & Wilson, L. (1987) *J. Cell Biol. 104*, 1035–1046.

Fendrick, J. L., & Iglewski, W. J. (1989) *Proc. Natl. Acad. Sci. U.S.A. 86*, 554–557.

Gill, D. M., & Meren, R. (1978) *Proc. Natl. Acad. Sci. U.S.A. 75*, 3050–3054.

Gilman, A. G. (1984) *Cell 36*, 577–579.

Grundke-Iqbal, I., Iqbal, K., Tung, Y.-C., Quinlan, M., Wisniewski, H. M., & Binder, L. I. (1986) *Proc. Natl. Acad. Sci. U.S.A. 83*, 4913–4917.

Hawkins, D. J., & Browning, E. T. (1982) *Biochemistry 21*, 4474–4479.

Hendershot, L. M., Ting, J., & Lee, A. S. (1988) *Mol. Cell. Biol. 8*, 4250–4256.

Kaslow, H. R., Groppi, V. E., Abood, M. E., & Bourne, H. R. (1981) *J. Cell Biol. 91*, 410–413.

Laemmli, U. K. (1970) *Nature 227*, 680–685.

Lee, H., & Iglewski, W. (1984) *Proc. Natl. Acad. Sci. U.S.A. 81*, 2703–2707.

Leno, G. H., & Ledford, B. E. (1989) *Eur. J. Biochem. 186*, 205–211.

Lim, L.-K., Sekura, R., & Kaslow, H. R. (1985) *J. Biol. Chem. 260*, 2585–2588.

Lindwall, G., & Cole, R. D. (1984) *J. Biol. Chem. 259*, 5301–5305.

Ludden, P. W., & Roberts, G. P. (1989) *Curr. Top. Cell. Regul. 30*, 23–52.

Margolis, R. L., Rauch, C. T., & Job, D. (1986) *Proc. Natl. Acad. Sci. U.S.A. 83*, 639–643.

Margolis, R. L., Whitten, R., Rauch, C. T., Hassain, H., & Smith, R. (1988) in *Amyotrophic Lateral Sclerosis* (Tsubaki, T., & Yasa, Y., Eds.) Elsevier, Amsterdam.

Moss, J., & Richardson, S. H. (1978) *J. Clin. Invest. 62*, 281–285.

Moss, J., & Vaughan, M. (1978) *Proc. Natl. Acad. Sci. U.S.A. 75*, 3621–3624.

Moss, J., Stanley, S. J., & Watkins, P. A. (1980) *J. Biol. Chem. 255*, 5838–5840.

O'Farrell, P. H. (1975) *J. Biol. Chem. 250*, 4007–4021.

Pfeuffer, T., & Helmreich, E. (1989) *Curr. Top. Cell. Regul. 29*, 129–216.

Raeburn, S., Goor, R., Schneider, J., & Maxwell, E. (1968) *Proc. Natl. Acad. Sci. U.S.A. 61*, 1428–1434.

Richter, C., Winterhalter, K. H., Baumhüter, S., Lötscher, H.-R., & Mosher, B. (1983) *Proc. Natl. Acad. Sci. U.S.A. 80*, 3188–3192.

Soman, G., Mickelson, J. R., Louis, C. F., & Graves, D. J. (1984) *Biochem. Biophys. Res. Commun. 120*, 973–980.

Sternlicht, H., Yaffe, M. B., & Farr, G. W. (1987) *FEBS Lett. 214*, 226–235.

Stewart, R. J., Farrell, K. W., & Wilson, L. (1990) *Biochemistry 29*, 6489–6498.

Tanigawa, Y., Tsuchiya, M., Imai, Y., & Shimoyama, M. (1984) *J. Biol. Chem. 259*, 2022–2029.

Tanuma, S., Kawashima, K., & Hiroyoshi, E. (1989) *J. Biol. Chem. 263*, 5485–5489.

Towbin, H., Staehelin, T., & Gordon, J. (1979) *Proc. Natl. Acad. Sci. U.S.A. 76*, 4350–4354.

Tsai, S., Adamik, R., Moss, J., Vaughan, M., Manne, V., & Kung, H. (1985) *Proc. Natl. Acad. Sci. U.S.A. 82*, 8310–8314.

Tsuyama, S., Bramblett, G. T., Huang, K.-P., & Flavin, M. (1986) *J. Biol. Chem. 261*, 4110–4116.
Tsuyama, S., Tereyama, Y., & Matsuyama, S. (1987) *J. Biol. Chem. 262*, 10886–10892.
West, R. E., Jr., & Moss, J. (1986) *Biochemistry 25*, 8057–8062.
Williams, R. C., & Detrich, H. W., III (1979) *Biochemistry 18*, 2499–2503.
Ueda, K., & Hayaishi, O. (1985) *Annu. Rev. Biochem. 54*, 73–100.

CORRECTIONS

Nuclear Matrix Bound V(D)J Recombination Activity in Rat Thymus Nuclei: An in Vitro System, by V. P. Dave, M. J. Modak, and V. N. Pandey*, Volume 30, Number 19, May 14, 1991, pages 4763–4767.

We reported that nuclear matrix isolated from young rat thymus contained an activity that supported V(D)J recombination in vitro at high efficiency. This conclusion was based on the observation that a plasmid substrate (pJH200), when treated with matrix and transfected into *E. coli*, gave rise to ampicillin- and chloramphenicol-resistant colonies. Subsequent restriction enzyme (*Agi*A1, *Pvu*II, and *Sal*I) mapping analyses of the recombined plasmid, however, clearly suggest that the double antibiotic resistance is not a consequence of V(D)J signal sequence directed recombination (unpublished results). Therefore, the earlier interpretation of successful V(D)J recombination in vitro is erroneous.

Structure of the Smooth Muscle Myosin Light-Chain Kinase Calmodulin-Binding Domain Peptide Bound to Calmodulin, by Sharon M. Roth, Diane M. Schneider, Laura A. Strobel, Mark F. A. VanBerkum, Anthony R. Means, and A. Joshua Wand*, Volume 30, Number 42, October 22, 1991, pages 10078–10084.

The foundation defining the biological significance and behavior of the peptide used was inadequately summarized. Reference to a paper critical to the original definition and characterization of the smooth muscle myosin light-chain kinase calmodulin-binding domain was inadvertently omitted. The citations should have included the following: Lukas, T. J., Burgess, W. H., Prendergast, F. G., Lau, W., & Watterson, D. M. (1986) *Biochemistry 25*, 1458–1464.

Structural Determination of Oligosaccharides Derived from Lipooligosaccharide of *Neisseria gonorrhoeae* F62 by Chemical, Enzymatic, and Two-Dimensional NMR Methods, by Ryohei Yamasaki,* Bradley E. Bacon, Wade Nasholds, Herman Schneider, and J. M. Griffiss, Volume 30, Number 43, October 29, 1991, pages 10566–10575.

The identity of the heptose in the text was quoted to be L-*glycero*-D-*manno*-heptose on the basis of the results obtained by high-performance anion-exchange chromatography and NMR. However, the J coupling data ($J_{2,3}$, $J_{3,4}$, $J_{4,5}$) indicate that the stereochemistry of the carbohydrate ring structure of the two heptoses is not manno but talo if the ring structure is in the $^4C_1$ conformation. Since the ring conformation of the *manno*-heptose could be different from the $^4C_1$ conformation, we cannot rule out the possibility that the Hep has a manno configuration. Currently, the identity of the Hep is under investigation.